Mesh-independent topology optimisation in the H^1 Sobolev space

Michal Habera[1], Johannes Neumann[1], Jack S. Hale[2]

[1]Rafinex SARL, [2]University of Luxembourg

About Rafinex SARL

- based in Luxembourg, Berlin and London,
- development of cloud-based topology optimization software called Möbius,
- features: stochastic optimization for robust designs, **adaptive anisotropic mesh refinement**, manufacturing constraints, stress constraint, web based GUI.

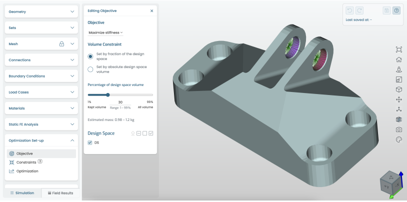

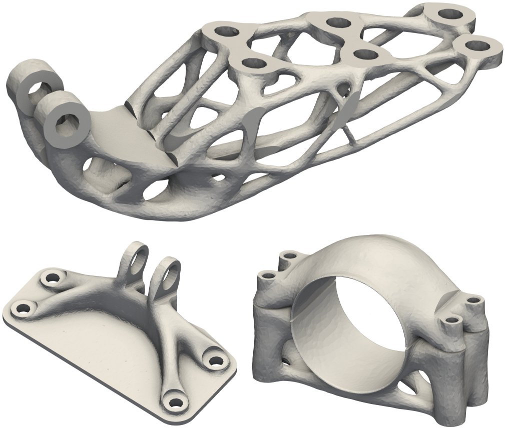

Find $u \in U(\Omega), \varphi \in V(\Omega)$, s.t.

$$
\begin{aligned}
\min C(u) = \min \int_\Omega f \cdot u \, \mathrm{d}s, \\
\varphi \in [\delta, 1], \\
\int_\Omega \varphi \, \mathrm{d}x - \mathsf{Vol} = 0, \\
\int_\Omega \varepsilon(u) : \mathsf{E}(\varphi)\varepsilon(v) \, \mathrm{d}x = \int_\Gamma f \cdot v \, \mathrm{d}s, \quad \forall v \in U(\Omega)
\end{aligned}
$$

Topology Optimization for minimum compliance 1

Find $u \in U(\Omega), \varphi \in V(\Omega)$, s.t.

$$\min C(u) = \min \int_\Omega f \cdot u \, \mathrm{d}s,$$

$$\varphi \in [\delta, 1],$$

$$\int_\Omega \varphi \, \mathrm{d}x - \mathsf{Vol} = 0,$$

$$\int_\Omega \varepsilon(u) : \mathsf{E}(\varphi)\varepsilon(v) \, \mathrm{d}x = \int_\Gamma f \cdot v \, \mathrm{d}s, \quad \forall v \in U(\Omega)$$

i.e., find critical points of the Lagrange functional $\mathcal{L}$,

$$\mathcal{L}(\varphi, u, v, \lambda) = C(u) - \left(\int_\Omega \varepsilon(u) : \mathsf{E}(\varphi)\varepsilon(v) \, \mathrm{d}x - \int_\Gamma f \cdot v \, \mathrm{d}s \right) + \lambda \left(\int_\Omega \varphi \, \mathrm{d}x - \mathsf{Vol} \right),$$

+ bounds constraint. SIMP penalization $\mathsf{E}(\varphi) = \varphi^p \mathsf{E}_0$.

Regularization techniques

- local or global slope (gradient) constraints, which add a bound on the spatial gradient of the density,
- phasefield or diffused interface formulations, where Landau-Ginzburg functional is considered in order to introduce a finite transition layer,
- $W^{1,p}$ and Tikhonov regularization methods where an L^p norm of spatial gradient is added as additional objective term,
- density filtering which formulates the optimization problem in terms of filtered density $\hat{\varphi} = \mathcal{F}(\varphi)$, where $\mathcal{F}$ is a filter operator,

- local or global slope (gradient) constraints, which add a bound on the spatial gradient of the density,
- phasefield or diffused interface formulations, where Landau-Ginzburg functional is considered in order to introduce a finite transition layer,
- $W^{1,p}$ and Tikhonov regularization methods where an L^p norm of spatial gradient is added as additional objective term,
- density filtering which formulates the optimization problem in terms of filtered density $\hat{\varphi} = \mathcal{F}(\varphi)$, where $\mathcal{F}$ is a filter operator,
- sensitivity filters, where functional gradient is heuristically filtered using a filter operator, $\widehat{\nabla \mathcal{L}} = \mathcal{F}(\nabla \mathcal{L})$.

$$\mathrm{d}\mathcal{L}(v;\delta v) = -\int_\Omega \varepsilon(u) : \mathsf{E}(\varphi)\varepsilon(\delta v)\,\mathrm{d}x + \int_\Gamma f\cdot\delta v\,\mathrm{d}s = 0, \quad \forall \delta v \in U(\Omega), \quad \text{(state equation)}$$

$$\mathrm{d}\mathcal{L}(u;\delta u) = \int_\Gamma f\cdot\delta u\,\mathrm{d}s - \int_\Omega \varepsilon(\delta u) : \mathsf{E}(\varphi)\varepsilon(v)\,\mathrm{d}x = 0, \quad \forall \delta u \in U(\Omega), \quad \text{(adjoint equation)}$$

$$\mathrm{d}\mathcal{L}(\lambda;\delta\lambda) = \delta\lambda\left(\int_\Omega \varphi\,\mathrm{d}x - \mathsf{Vol}\right) = 0, \quad \forall \delta\lambda \in \mathbb{R},$$

$$\mathrm{d}\mathcal{L}(\varphi;\delta\varphi) = -\int_\Omega \varepsilon(u) : \frac{\partial\mathsf{E}}{\partial\varphi}\varepsilon(v)\delta\varphi\,\mathrm{d}x + \lambda\int_\Omega \delta\varphi\,\mathrm{d}x = 0, \quad \forall \delta\varphi \in V(\Omega).$$

Gradient interpretation and Riesz representation 1

Sensitivity of the reduced functional

$$\frac{\partial \mathcal{L}}{\partial \varphi} = -\varepsilon(u) : \frac{\partial \mathsf{E}}{\partial \varphi} \varepsilon(v) + \lambda$$

$$\varphi_1 = \varphi_0 - \alpha \frac{\partial \mathcal{L}}{\partial \varphi}$$

Gradient interpretation and Riesz representation 1

Sensitivity of the reduced functional

$$\frac{\partial \mathcal{L}}{\partial \varphi} = -\varepsilon(u) \colon \frac{\partial \mathsf{E}}{\partial \varphi} \varepsilon(v) + \lambda$$

$$\varphi_1 = \varphi_0 - \alpha \frac{\partial \mathcal{L}}{\partial \varphi}$$

Riesz representation theorem. Let H be a Hilbert space equipped with an inner product denoted $(\cdot, \cdot)_H$ and the induced norm $||u||_H := \sqrt{(u, u)_H}$. For every continuous linear functional $f \in H^*$ there exists a unique vector $u_f \in H$, called the *Riesz representation* of f, such that

$$f(x) = \left\langle x, u_f \right\rangle_H, \quad \forall x \in H. \tag{1}$$

The map $\mathcal{R}_H : H' \longrightarrow H$ is called the *Riesz map*.

Gradient interpretation and Riesz representation 2

Gradient Descent in Hilbert spaces

$$\varphi_1 = \varphi_0 - \alpha \mathcal{R}_V\big(D_\varphi \mathcal{L}\big)\,.$$

For the compliance functional there is

$$D_\varphi \mathcal{L}_C[\delta\varphi] = -\int_\Omega \varepsilon(u) \colon \frac{\partial \mathsf{E}}{\partial \varphi} \varepsilon(v) \delta\varphi \,\mathrm{d}x$$

and we denote

$$\nabla_\varphi \mathcal{L} = \mathcal{R}_V\big(D_\varphi \mathcal{L}\big)\,.$$

Gradient interpretation and Riesz representation 3

Let us consider $V(\Omega) := H^1_\kappa(\Omega)$ with the scalar product

$$\langle u, v\rangle_{H^1_\kappa} := \int_\Omega uv \,\mathrm{d}x + \kappa^2 \int_\Omega \nabla u \cdot \nabla v \,\mathrm{d}x.$$

Then $g \in H^1_\kappa(\Omega)$ s.t.

$$\int_\Omega g\tau \,\mathrm{d}x + \kappa^2 \int_\Omega \nabla g \cdot \nabla \tau \,\mathrm{d}x = -\int_\Omega \varepsilon(u) : \frac{\partial \mathsf{E}}{\partial \varphi} \varepsilon(v) \tau \,\mathrm{d}x$$

could be seen as sensitivity filter based on positive definite Helmholtz PDE.

Optimality Criteria 1

- Gradient Descent could be slow,
- Sequential Quadratic Programming methods costly,
- special case of SAO (Sequential Approximate Optimization), along with the MMA (Method of Moving Asymptotes),
- for the case of the compliance functional we know that it behaves locally as φ^{-1},

Optimality Criteria 1

- Gradient Descent could be slow,
- Sequential Quadratic Programming methods costly,
- special case of SAO (Sequential Approximate Optimization), along with the MMA (Method of Moving Asymptotes),
- for the case of the compliance functional we know that it behaves locally as φ^{-1},

$$\mathcal{L} \approx \mathcal{L}_{\text{rec}}(\varphi) = \mathcal{L}(\varphi_0) + \langle \varphi - \varphi_0, \nabla_\varphi \mathcal{L} \rangle_{L^2} + \frac{1}{2} \left\langle \varphi - \varphi_0, \frac{-2\nabla_\varphi \mathcal{L}_C}{\varphi}(\varphi - \varphi_0) \right\rangle_{L^2} =$$

$$\ldots + \frac{1}{2} \langle \varphi - \varphi_0, H(\varphi - \varphi_0) \rangle_{L^2}$$

where the Hessian approximation $H = \frac{-2\nabla_\varphi \mathcal{L}_C}{\varphi}$.

Optimality

$$\mathrm{d}\mathcal{L}_{\text{rec}}(\varphi;\delta\varphi) = 0, \quad \forall \delta\varphi \in V(\Omega)$$

of the above leads to: find $\varphi \in V(\Omega)$, s.t.

$$\int_\Omega \left(\lambda + \nabla_\varphi \mathcal{L}_C \frac{\varphi_0^2}{\varphi^2}\right) \delta\varphi \,\mathrm{d}x = 0, \quad \forall \delta\varphi \in V(\Omega),$$

which suggests

$$\varphi_1 = \left(\frac{-\nabla_\varphi \mathcal{L}_C}{\lambda}\right)^{1/2} \varphi_0.$$

Alternatively, we take constant Hessian approximation based on previous iterate

$$H = \frac{-\gamma \nabla_\varphi \mathcal{L}_C}{\varphi_0}.$$

which would be satisfied for

$$\varphi_1 = \left(\frac{(1+\gamma)}{\gamma} + \frac{\lambda}{\gamma \nabla_\varphi \mathcal{L}_C} \right) \varphi_0.$$

- quadratic approximation

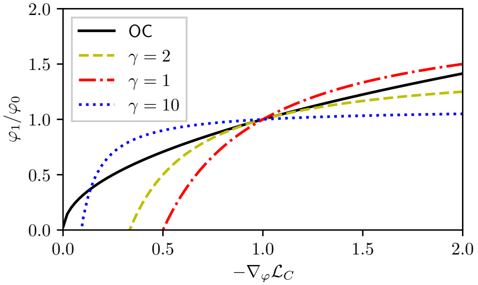

Figure 1: Comparison of the traditional OC method with the OC method based on quadratic approximation.

Optimality Criteria 4

Traditional results on the existence of minimizers for the SIMP scheme work for the following assumptions (not exclusive)

- set of admissible densities is bounded in H^1,
- SIMP exponent $p < d/(d-2)$,
- set of displacement solutions for all admissible densities is bounded in $[H_0^1]^d$.

Set of admissible densities is bounded in H^1?

Optimality Criteria 4

Traditional results on the existence of minimizers for the SIMP scheme work for the following assumptions (not exclusive)

- set of admissible densities is bounded in H^1,
- SIMP exponent $p < d/(d-2)$,
- set of displacement solutions for all admissible densities is bounded in $[H_0^1]^d$.

Set of admissible densities is bounded in H^1?

- add Tikhonov penalty term to the reciprocal approximation

$$\mathcal{L}_{\text{tikh}} = \mathcal{L}_{\text{rec}} + \frac{\alpha}{2} \langle \nabla\varphi, \nabla\varphi \rangle_{L^2}$$

- explicit expression for $\varphi_1 = (\ldots)\,\varphi_0$ does not exist, since Optimality Criteria step is now a PDE.

Algorithm summary

Start $\varphi_0 = 0.5$;
while $||\varphi_{k+1} - \varphi_k||_{H^1_\kappa} > 10^{-2}$ **do**
  Find u_k, solve state equation
  $\mathbf{K}(\varphi_k)u_k = f$;
  $v_k \leftarrow u_k$;
  Find g_k, solve Riesz representation
  $\mathbf{H}g_k = D_\varphi \mathcal{L}_C$;
  Estimate $\lambda_{\text{min}}, \lambda_{\text{max}}$;
  while *volume constraint* $> 10^{-8}$ **do**
    Find φ^*_{k+1}, solve Optimality Criteria;
    Project into (box) bounds constraint,
    $\varphi_{k+1} \leftarrow \mathcal{P}(\varphi^*_{k+1})$;
  end
  $k \leftarrow k+1, \varphi_k \leftarrow \varphi_{k+1}$
end

Toolchain:

- `gmsh`, triangular/tetrahedral mesh generation,
- `FEniCSx`, FEM assembly and MPI mesh parallelism,
- `PETSc`, matrix solvers,
  - GMRES+GAMG,
  - CG+Jacobi,
- `ParaView`, visualization.

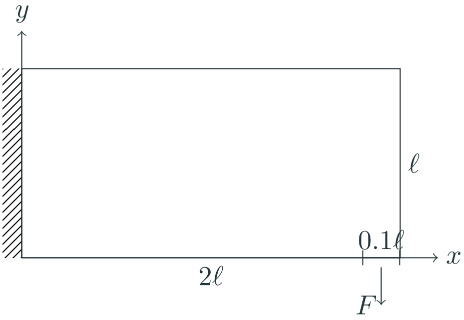

Figure 2: Cantilever beam setup.

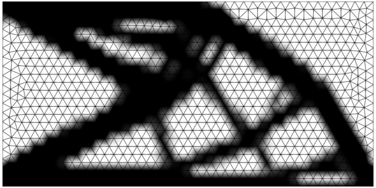

(a) $^*\kappa = 0$.

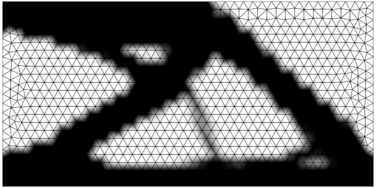

(b) $\kappa = 0.05\ell$.

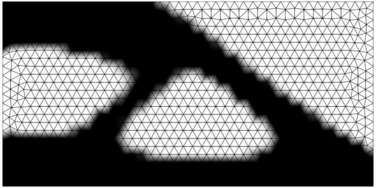

(c) $\kappa = 0.2\ell$.

Figure 3: The effect of Riesz scale parameter κ on the optimal design in the cantilever beam example, $\alpha = 0$.

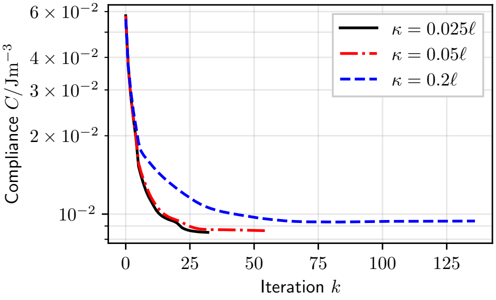

(a) Compliance.

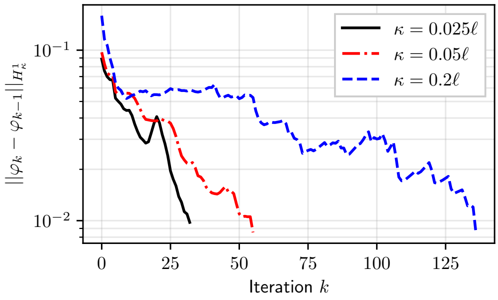

(b) H^1_κ norm of the difference between consecutive iterations.

Figure 4: Convergence of the OC method for the cantilever beam problem.

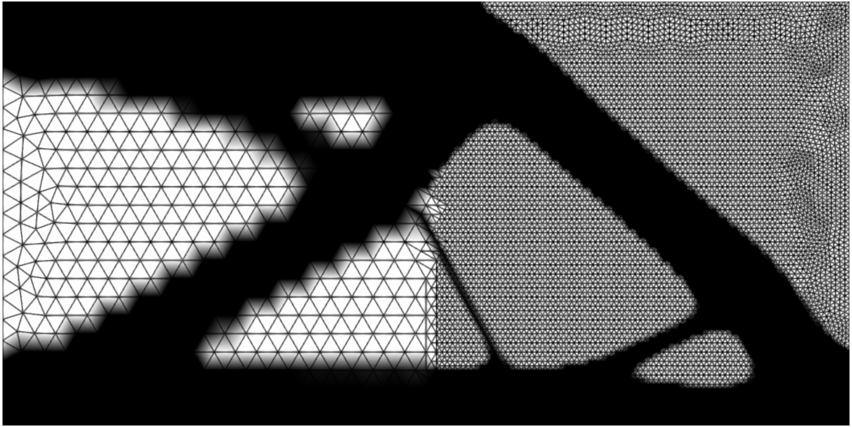

Figure 5: Mesh-independent optimal cantilever beam topology for locally refined mesh ($x > 0.5\ell$), $\kappa = 0.05\ell$ and $\alpha = 0$.

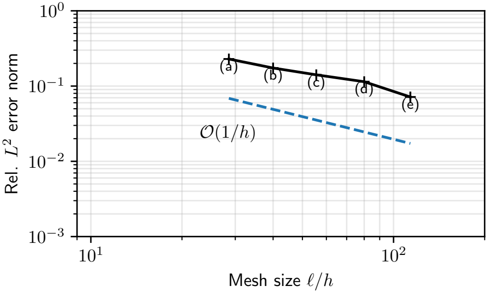

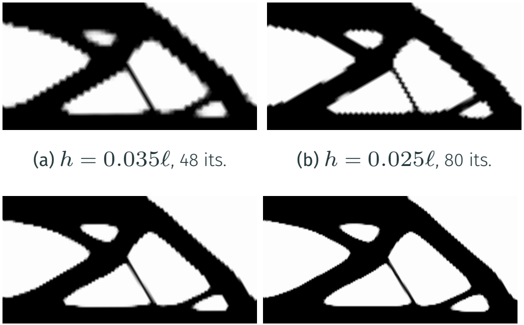

(a) $h = 0.035\ell$, 48 its.

(b) $h = 0.025\ell$, 80 its.

(c) $h = 0.018\ell$, 88 its.

(d) $h = 0.0125\ell$, 96 its.

Figure 6: Convergence of the cantilever optimal solution under uniform mesh refinement for a fixed $\kappa = 0.05\ell$, $\alpha = 0$.

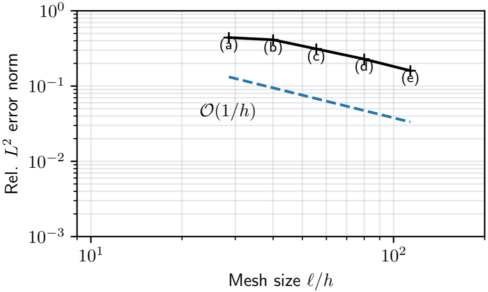

(a) $h = 0.035\ell$, 37 its.

(b) $h = 0.025\ell$, 49 its.

(c) $h = 0.018\ell$, 49 its.

(d) $h = 0.0125\ell$, 56 its.

Figure 7: Convergence of the cantilever optimal solution under uniform mesh refinement for $\kappa = h$, $\alpha = 0$.

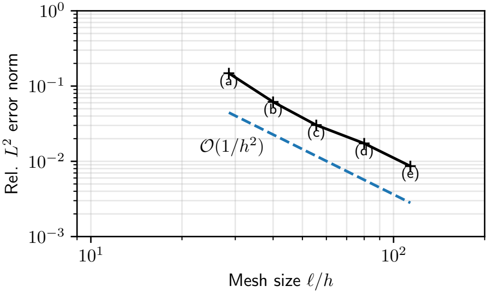

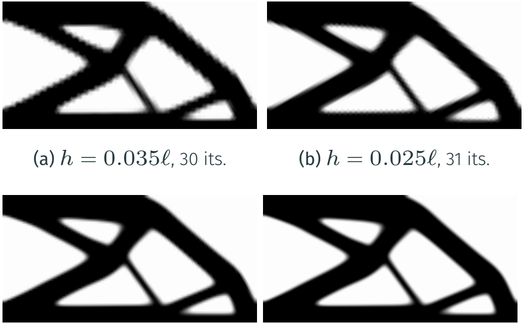

(a) $h = 0.035\ell$, 30 its.

(b) $h = 0.025\ell$, 31 its.

(c) $h = 0.018\ell$, 32 its.

(d) $h = 0.0125\ell$, 32 its.

Figure 8: Convergence of the cantilever optimal solution under uniform mesh refinement for $\kappa = 0.02\ell, \alpha = 0.002\ell$.

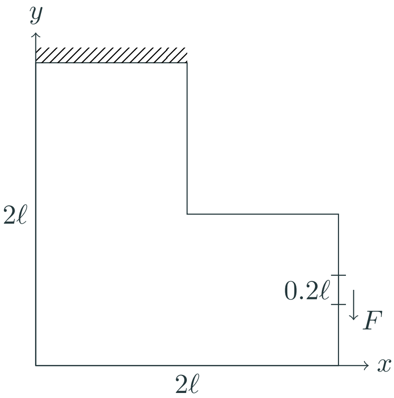

Figure 9: L-shape beam setup.

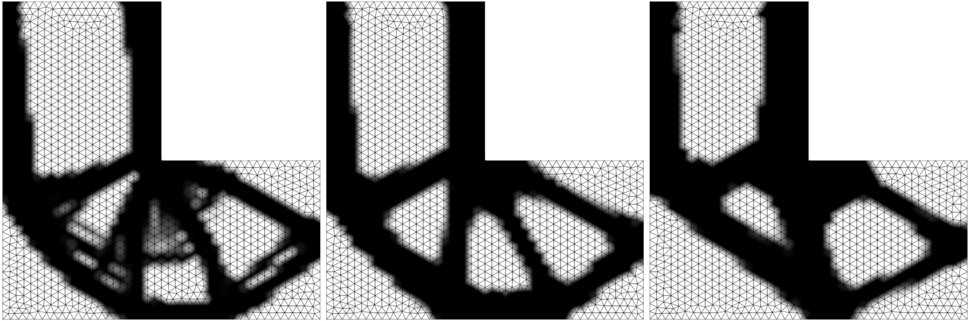

(a) $^{*}\kappa = 0$. (b) $\kappa = 0.05\ell$. (c) $\kappa = 0.2\ell$.

Figure 10: The effect of Riesz scale parameter κ on the optimal design in the L-shape beam example, $\alpha = 0$.

Example: L-shape

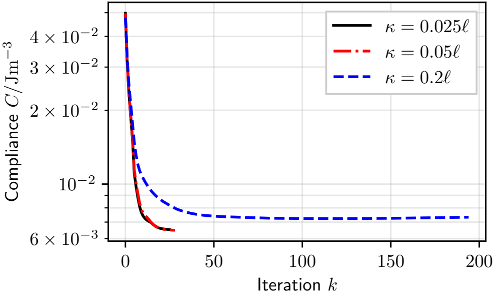

(a) Compliance.

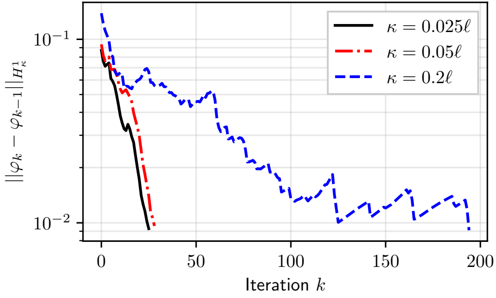

(b) H^1_κ norm of the difference between consecutive iterations.

Figure 11: Convergence of the OC method for the L-shape beam problem.

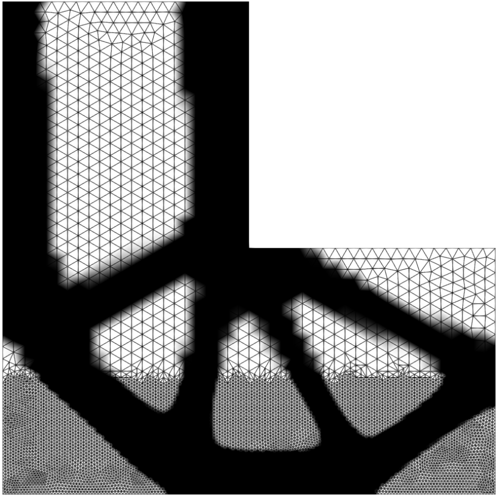

Figure 12: Mesh-independent optimal L-shaped beam topology for locally refined mesh ($y < 0.25\ell$), $\kappa = 0.05\ell$, $\alpha = 0$.

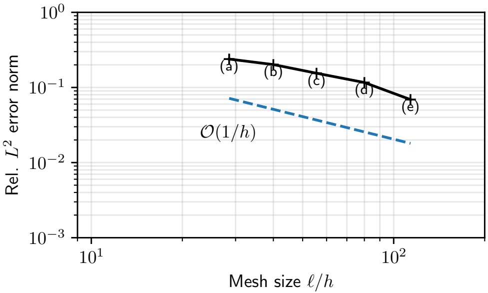

(a) $h = 0.035\ell$, 51 its.

(b) $h = 0.025\ell$, 63 its.

(c) $h = 0.018\ell$, 93 its.

(d) $h = 0.0125\ell$, 114 its.

Figure 13: Convergence of the L-shape optimal solution under uniform mesh refinement for a fixed $\kappa = 0.05\ell$, $\alpha = 0$.

Example: L-shape

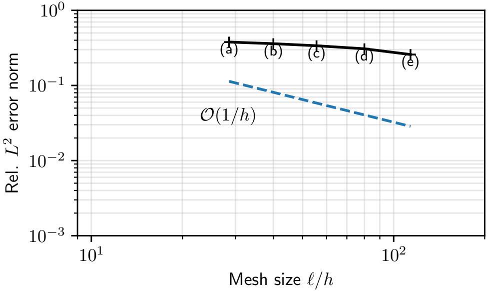

(a) $h = 0.035\ell$, 37 its.

(b) $h = 0.025\ell$, 40 its.

(c) $h = 0.018\ell$, 35 its.

(d) $h = 0.0125\ell$, 36 its.

Figure 14: Convergence of the L-shape optimal solution under uniform mesh refinement for $\kappa = h$, $\alpha = 0$.

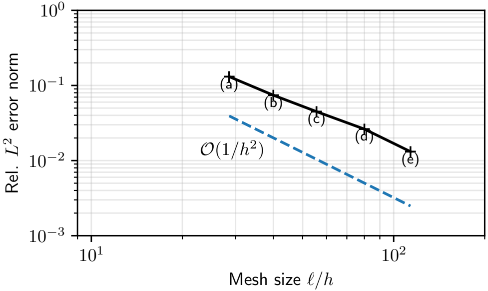

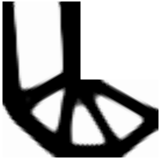

(a) $h = 0.035\ell$, 27 its.

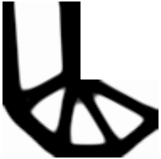

(b) $h = 0.025\ell$, 30 its.

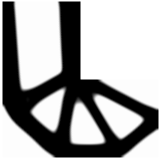

(c) $h = 0.018\ell$, 32 its.

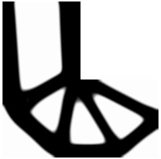

(d) $h = 0.0125\ell$, 34 its.

Figure 15: Convergence of the cantilever optimal solution under uniform mesh refinement for $\kappa = 0.02\ell, \alpha = 0.002\ell$.

Example: L-shape

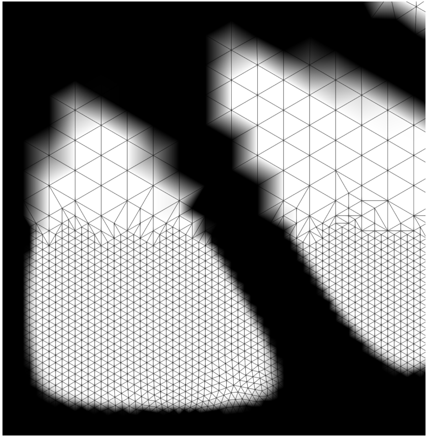

(a) $\alpha = 0$.

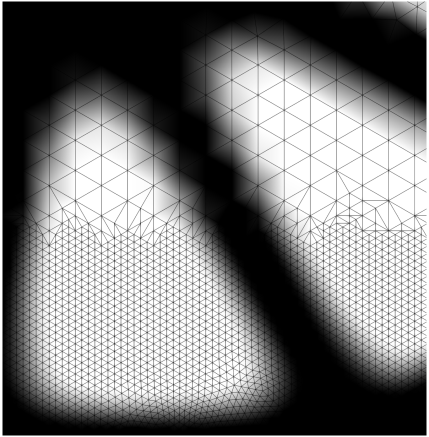

(b) $\alpha = 0.003\ell$.

Figure 16: Independent diffused interface thickness and “feature size” control.

Summary

- density-based compliance TO formulated in H^1_κ,
- Helmholtz sensitivity filter interpreted as Riesz map,
- efficient OC-like reciprocal Hessian approximation,
- 2D mesh convergence study.

The present project is supported by the National Research Fund, Luxembourg, under Industrial Fellowship project ”COAT”, Ref. 17205623.